



Original Article

Impact assessment of climatic condition on rangeland vegetation cover through

RS and GIS techniques

S.Poormohammadi^{1*}
M.H.Rahimian²
M.Kalantar³
S.Poormohammadi⁴

Received Date: May/7/2011
Accepted Date: Mar/23/2011

Abstract

In this study an indicator was introduced, namely “impact factor” (I). It shows impacts of long term climatic conditions on rangeland vegetation status. It considers precipitation and temperature as two main climatic parameters and also a remotely sensed vegetation index, SAVI. The impact factor was successfully implemented in this case study through integration of MODIS time series and eight meteorological station records. Also digital elevation model (DEM) was employed as an ancillary data for interpolation and generation of temperature and precipitation maps. In the studied region, northern areas which were also the plain outlet showed the maximum “I” values compared with other areas. These areas were found more susceptible to degradation of their resources (vegetation cover) as direct impacts of climatic conditions and drought spells.

Keywords: MODIS, Vegetation Cover, Climate, Rangeland, Impact Factor

1-Islamic Azad University, Yazd, Iran ,
Young Research Club, MSc. of desert
management

2-rrigation and drainage expert, RS & GIS
dept., National Salinity Research Center
(NSRC), Yazd, Iran,

3-Faculty member, Islamic Azad
University, Yazd, Iran,

4-MSc student, Shahid Bahonar
University, Kerman, Iran
s.poormohammadi@gmail.com

INTRODUCTION

Rangeland is a type of land which is characterized by non-forest, native vegetation [NRCS, 1997]. Types of land cover in a rangeland are grasslands, shrub lands, and savannas, which are determined by climate. Healthy rangelands are a national resource that will sustain soil quality, enhance the availability of clean water, sequester excess carbon dioxide, maintain plant and animal diversity, and support a myriad of other non-agricultural uses [Follett et al., 2001]. Generally, yearly variability of precipitation make rangelands unsuitable for crop production, and livestock grazing presents a sustainable means of food and fiber production [Hunt et al, 2003]. Droughts, may drastically affect plant community composition and make rangelands more susceptible to diseases, insect pests, weed invasions, and overgrazing. Continuous monitoring of rangeland status seems to be necessary and useful in this field. It would

help decision makers to do necessary interventions and adopt proper measure against drought spells.

Current ground-based methods are not suitable for regional assessments and monitoring of rangelands, seasonality. These methods invariable consume plenty of time and expense. Conversely, satellite remote sensing [RS] techniques can provide useful information about changes of rangeland status due to changes in climatic attributes of the region [Lunetta et al, 2006]. This technique is significantly promising for the development of more reliable and economically feasible measures of vegetation status over large areas. This technique can monitor vegetation cover status both in time and space [Tueller 1989]. In fact, monitoring of large areas at low cost and a relatively low time span is the forte of remote sensing technique.

Successful application of this technique for the monitoring of rangeland would be attainable with the help of vegetation indices [Bhaskar et al, 1994; Hunsaker, 2005]. Vegetation indices [VI] represent different combinations between red [R] and near infrared [NIR] portions of the spectrum [bands]. Green vegetative surfaces strongly absorb red light and strongly reflect near-infrared energy. No other materials have this spectral signature [Lillesand and Keifer, 2000]. Many Red-NIR combinations have been proposed on this basis [Tucker 1979; Lyburner et al. 2000].

Furthermore, drought is a climatic phenomenon that influences green vegetation and in addition, water is one of the most common limitations that cause this phenomenon. Therefore, remote sensing of vegetation water content can play an important role in monitoring of drought impacts on rangeland vegetation. Besides the thermal region of the electromagnetic spectrum [8–14 μ m], two spectral regions have been found to be suitable for detection of plant water content: the near-infrared region [NIR, 0.7–1.3 μ m] and the shortwave infrared region [SWIR, 1.3–2.5 μ m] [Reeves et al., 2002].

NDVI [Normalized Difference Vegetation Index] is one of the most frequently used vegetation indices for monitoring of moisture-related vegetation condition. It calculates as $[\rho_{\text{NIR}} - \rho_{\text{RED}}]/[\rho_{\text{NIR}} + \rho_{\text{RED}}]$, where ρ_{RED} and ρ_{NIR} are radiances in red and near infra red portions of the spectrum, respectively.

Estimation of standing dry mass and yields was one of the earliest applications of satellite remote sensing for agricultural crops, and the developed techniques were applied early on to rangelands [Tucker et al., 1975; Richardson et al., 1983; Everitt et al., 1986; Aase et al., 1987; Anderson et al., 1993b]. At the time, field techniques for estimating productivity were based on measuring peak biomass, so estimation of productivity for rangelands was based on remote sensing peak biomass [Tucker et al., 1983; Everitt et al., 1989]. However, two main approaches have been followed for the purpose of rangeland monitoring through RS data. Establishment of direct empirical relationships between spectral reflectance of land cover and its biomass is one the approaches that have been accomplished by some researchers [e.g. Tucker et al. 1983 and Wylie et al. 1995]. In the second approach, spectral reflectance data have been used to derive different vegetation indices and also other vegetation related parameters. In this regard, numerous broad scale studies [Thoma 1998, Tucker et al. 1983, Kennedy 1989 and Merril et

al. 1993] have shown that live biomass of a rangeland is correlated to remotely sensed vegetation indices, particularly NDVI. Also leaf area index [LAI] is related to mass of the foliage; the ratio between leaf area and leaf mass is the specific leaf area. Many studies examined the use of remote sensing for estimating LAI [Curran, 1983; Hatfield et al., 1985; Price, 1993; Price and Bausch, 1995; Qi et al., 2000c]. Absorbed photosynthetically active radiation [APAR] also was found suitable for estimation of rangeland biomass [Choudhury 1987]. However, the second approaches are likely to be more successful in predicting rangeland status across different climatic conditions. But some problems became apparent, which limits the usefulness of these approaches. One of the major limitations refers to soil background. It has strong effects on remotely sensed data [Ezra et al., 1984; Huete et al, 1985; Huete, 1988; Price, 1993; Qi et al., 1994; Price and Bausch, 1995] and forces the established equations to be site specific. However, multi temporal remote sensing is powerful and allows more mechanistic models of plant production to be used because, in part, the soil background is constant [Hunt et al, 2003]. Data from the Landsat Thematic Mapper [TM4 and TM5] and the Enhanced TM plus [Landsat 7] are suitable for rangeland management [Nouvellon et al., 2000; Nouvellon et al., 2001] because the 20-year time series of these data can be averaged to overcome the high year-to-year variation from precipitation [Hunt et al, 2003]. With Landsat Multispectral Scanner [Landsat 1 to 5] data, the time series of data extends to 30 years. Long time series of these data type have been used by Washington-Allen et al. [1999] to examine plant community changes in relation to climatic variability. Also in most applications, remotely sensed imagery has been merged with other images or geospatial data such as Digital Elevation Model [DEM], records of meteorological stations, soil maps and field observations of some rangeland attributes.

In the present study a time series of Moderate Resolution Imaging Spectroradiometer [MODIS] data have been used to monitor rangeland status in ten successive years, and also to investigate the impact of climatic parameters on vegetation cover and its variability in the rangeland. MODIS was successfully deployed by NASA on 18, December 1999. Several decades of improved communications, hardware, software, data storage capacity, and satellite engineering enable the MODIS instrument to provide enhanced monitoring capabilities. A suite of satellites has been used to measure and monitor biophysical

constituents of the earth's surface, each exhibiting different characteristics. The MODIS sensor, however, is unique because it combines both the spatial and spectral resolution of several satellites on a single platform [Hunt et al, 2003]. MODIS presents greater radiometric resolution than traditional sensors providing a broader range of measurement and therefore increased sensitivity to small changes in spectral reflectivity. The MODIS has 36 spectral bands, as compared to 5 on the AVHRR instrument, 7 on Landsat TM or 8 on the Landsat ETM+.

MATERIAL & METHODS

Study area is Yazd-Ardakan plain in Yazd province, in central Iran. This area lies between 53° 19' 33" to 55° 00' 28" east longitudes and 31° 12' 31" to 32° 39' 27" north latitudes. This plain is surrounded by Shirkouh mountain ranges in south and west, Kharanaq Mountain in east and Siahkouh playa in north. The Siahkouh playa is also the plain outlet. Total area of Yazd-Ardakan plain is 11630 square kilometers with elevations between 3240 and 990 m above sea level.

In this study 36 cloud free images were taken for derivation of ten well-known vegetation indices. These images were acquired from the MODIS sensor of Terra satellite in the first decade of 21st century [2000 to 2009]. Additionally, a Landsat ETM+ image was used for preparation of land use map and also interpretations due to its good spatial resolution [30 m]. [Table 2] represents the list of employed time series of satellite images.

Primarily, a correction approach was performed to convert pixel values of MODIS original data [or scaled integers, SI] to reflectance values for Red and NIR, separately. This approach is based on calculation of different indicators namely eccentricity correction factor, equation of time, local apparent time, hour angle, solar declination, cosine of solar zenith angle and earth sun distance for calibration of reflectance and radiance bands, respectively and finally correction of reflectance bands [Mokhtari, 2005]. After preparation of corrected reflectance bands [R and NIR], different vegetation indices [VI] were derived to monitor vegetation cover status in monthly and yearly time intervals [refer to [Table 2] to see the accurate time intervals]. Also [Table 3] shows list of employed indices with their calculation formulas.

Using updated land use map of the region, rangeland areas were identified and then, different VI values were extracted via crossing operation in ILWIS software. Mean VIs of Yazd-Ardakan rangeland for each image acquisition date then were calculated.

Accordingly, at least three VI datasets for April, May and June were prepared in different years. Month with maximum values of these VIs was identified and registered as representative month of that year. Finally, a dataset including mean VI values of representative months for ten successive years [2000-2009] was generated.

Identifying relationships between climatic attributes and rangeland vegetation status was accomplished in the next stage. In this stage, records of eight meteorological stations [Table 1] were collected for 2000-2009 time period. Precipitation [P], temperature [T], relative humidity [H], wind speed [W] and standardized precipitation index [SPI] were selected as the main climatic indicators of the region. Correlations between yearly values of these climatic parameters and different vegetation indices were established using R² correlation matrix. Through this procedure, fair correlations were investigated and therefore, the best vegetation index was identified. This index then was used for monitoring of drought impact on Yazd-Ardakan rangeland vegetation.

Precipitation and temperature maps of the studied region also were generated using gradients between Digital Elevation Model [DEM], P and T values of meteorological stations.

To investigate and monitor the impact of main climatic attributes [P and T] on rangeland vegetation cover status a rationale relationship was defined as follow:

$$I = f \left[\frac{T}{P * VI} \right]$$

Where, I is impact factor and shows pressure of climatic condition on rangeland vegetation status. It considers P and T as two main climatic parameters. As was mentioned before, P and T have been distinguished via a correlation analysis approach. VI in this formula is the selected remotely sensed vegetation index that can appropriately represent vegetation status of the studied rangeland. Therefore, to generate an impact factor map for the entire rangeland of the studied region, averaged maps of T, P and VI would be necessary for this incorporation via GIS approach capabilities. Based on this rationale relationship, regions with high values of impact factor [I] would be more susceptible for degradation of their resources [vegetation cover] as direct impacts of main climatic attributes. In this case study, impact factor map has been generated and classified

into three different levels [low, medium and high] and then interpreted, visually.

RESULTS & DISCUSSION

[Table 4] shows the matrix of correlation coefficients [R^2 statistics] between different climatic parameters and vegetation indices of Yazd-Ardakan rangeland. These values have been extracted through crossing operation between maps of P, T, H, WS, SPI and different vegetation index maps. Referring to this table, SAVI has the highest correlations with P, T and SPI. These climatic parameters and vegetation indices also are interrelated. For example, fair correlations exist between SAVI and PVI or fPAR [$R^2=0.60$ and $R^2=0.46$, respectively]. It means that SAVI is similar to PVI and fPAR, originally. Of which, SAVI was found better for this study. In fact, SAVI is the soil adjusted vegetation index that minimizes soil background effects.

Correlation coefficient between P and SPI also is significant [$R^2=1$]. The SPI index has originated from precipitation. This similarity led to elimination of SPI from the analysis procedure.

Figure 2 illustrates changes of annual precipitation and SAVI during 2000 to 2009. As shown in this figure, good agreements exist between temporal changes of these two indicators. It means that vegetation cover status in the studied rangeland is highly depended upon annual precipitation.

Finally, maps of SAVI, P and T [Figure 3] were integrated using the introduced relationship and ILWIS software capabilities. As a preliminary result, impact factor [I] map of Yazd-Ardakan plain was generated.

Figure 4[a] shows impact factor map of Yazd-Ardakan plain. "I" value in this map changes from 0.005 to 17.32, spatially. As shown in this map, lower "I" values belong to bordered areas in east, west and south. Northern areas have the higher "I" values, dominantly. As was mentioned before, regions with high values of impact factor [I] would be more susceptible for degradation of their vegetation cover. In the studied region, northern areas which are also the plain outlet [see figure 1] have the maximum "I" values compared with other areas. Spatially, lower part of Yazd-Ardakan plain [its outlet] is a region with minimum agricultural and pastoral activities due to its degraded soil and water resources, salinization, harsh climatic conditions and poor natural vegetations.

Visual interpretation of impact factor map also suggests three separate geographical areas in the plain. Based on this interpretation, regions with

low, medium and high impact factor values were extracted and illustrated in figure 4[b]. Results show that occupied areas for low, medium and high classes are 13%, 38% and 49% of total area, respectively.

To investigate the impact factor of Yazd-Ardakan rangeland, the "I" map was crossed with updated land use map of the plain. Figure 5[a] illustrates this map for rangeland areas. As shown in this figure, the impact factor ranges from 0.005 to 13.76. Figure 5[b] also presents classified impact factor map for Yazd-Ardakan rangeland. The results show that about 23%, 59% and 18% of total area belong to low, medium and high impact factors, respectively.

As shown in these maps, lower values for "I" belong to bordered areas, spatially. These areas are high elevated regions with relatively cold winters and moderate summers. In contrast, areas with high impact factors are generally located in low elevated rangelands, near to the foothills and desert areas of the plain. Major grazing activities also have focused on this region due to its moderate land slope, distance from water and to population centers. Therefore, it seems that areas with high impact factor values that are the consequence of both harsh climatic condition and low vegetation surfaces can significantly influence grazing activities in the rangeland. Consequently, vegetation cover in this region is at risk of degradation in upcoming decades.

CONCLUSION

In this study an indicator was introduced, namely "impact factor" [I]. It shows pressure of climatic conditions on rangeland vegetation status. It considers precipitation and temperature as two main climatic parameters and also a remotely sensed vegetation index, SAVI. The impact factor was successfully implemented in this case study through integration of MODIS time series and eight meteorological station records. Also digital elevation model [DEM] was employed as an ancillary data for interpolation and generation of temperature and precipitation maps. In the studied region, northern areas which were also the plain outlet had the maximum "I" values compared with other areas. These areas were found to be more susceptible for degradation of their resources [vegetation cover] as direct impacts of climatic conditions and drought occurrences.

The impact factor map can be used by researchers; decision makers and stakeholders for doing necessary interventions and for the purpose of sustainable rangeland management. It also can be interpreted and used based on other related

aspects such as grazing pattern, distance to water and population centers. Considering results of this case study, the introduced indicator was found suitable for monitoring of drought impact on rangeland vegetation and its classification. Repeatability and relatively low cost and time consumption are the major advantages of the introduced indicator.

ACKNOWLEDGMENT

This work was supported by a research project at Young Researchers' Club, Yazd branch of Azad University, Iran.

REFERENCE

- Aase, J.K., A.B. Frank, and R.J. Lorenz, 1987. Radiometric reflectance measurements of northern Great Plains rangeland and crested wheatgrass pastures, *Journal of Range Management*, 40:299–302.
- Anderson, G.L., J.D. Hanson, and R.H. Haas, 1993b. Evaluating Landsat Thematic Mapper derived vegetation indices for estimating above-ground biomass on semiarid rangelands, *Remote Sensing of Environment*, 45:165–175.
- Choudhury, B.J. 1987. Relationships between vegetation indices, radiation absorption, and net photosynthesis evaluated by a sensitivity analysis. *Remote Sensing Environ.* 22:209-233.
- Curran, P.J., 1983. Multispectral remote sensing for the estimation of green leaf area index, *Philosophical Transactions of the Royal Society of London, Series A*, 309:257–270.
- Everitt, J.H., M.A. Hussey, D.E. Escobar, P.R. Nixon, and B. Pinkerton, 1986. Assessment of grassland phytomass with airborne video imagery, *Remote Sensing of Environment*, 20:299–306.
- Everitt, J.H., D.E. Escobar, and A.J. Richardson, 1989. Estimating grassland phytomass production with near-infrared and midinfrared spectral variables, *Remote Sensing of Environment*, 30:257–261.
- Ezra, C.E., L.R. Tinney, and R.D. Jackson, 1984. Effect of soil background on vegetation discrimination using Landsat data, *Remote Sensing of Environment*, 16:233–242.
- Follett, R.F., J.M. Kimble, and R. Lal (editors), 2001. *The Potential of U.S. Grazing Lands to Sequester Carbon and Mitigate the Greenhouse Effect*, Lewis Publishers, Boca Raton, Florida, 442 p.
- Holfield, C.D., S. McElroy, M.S. Moran, R. Bryant, and T. Miura, in press. Temporal and spatial changes in grassland transpiration detected using Landsat TM and ETM₊ Imagery, *Canadian Journal of Remote Sensing*.
- Hunt E. R., Jr., J. H. Everitt, J. C. Ritchie, M. S. Moran, D. T. Booth, G. L. Anderson, P. E. Clark, and M. S. Seyfried, 2003, Applications and Research Using Remote Sensing for Rangeland Management, Photogrammetric Engineering & Remote Sensing, Vol. 69, No. 6, pp. 675–693.
- Hunt E. R., 2003. Leaf area index and cover of shortgrass steppe using AVIRIS imagery, *Proceedings of the Eleventh JPL Airborne Earth Science Workshop* (R.O. Green, editor), 05-08 March 2002, Pasadena, California (Jet Propulsion Laboratory,
- Hunsaker D. J., P. J. Pinter, Jr. Bruce, A. Kimball, 2005, Wheat basal crop coefficients determined by normalized difference vegetation index, *Irrig Sci* (2005) 24: 1–14.
- Huete, A.R., 1988. A soil-adjusted vegetation index (SAVI), *Remote Sensing of Environment*, 25:295–309.
- Huete, A.R., R.D. Jackson, and D.F. Post, 1985. Spectral response of a plant canopy with different soil backgrounds, *Remote Sensing of Environment*, 17:37–53.
- Jones, B.A., Ritters, K.H., Wickham, J.D., Tankersley Jr., R.D., O'Neill, R.V., Chaloud, D.J., Smith, E.R., & Neale, A.C. (1997). *An Ecological Assessment of the United States Mid-Atlantic Region: A Landscape Atlas*, U.S. Environmental protection Agency, Report No. EPA/600/R-97/130, U.S. Printing Office, Washington, DC, 104 p.
- Lunetta, R.L., Knight, F.K, Ediriwickrema, J., Lyon, J.G., and Worthy, L.D. (2006). Landcover change detection using multi-temporal MODIS NDVI data. *Remote Sensing of Environment*, 105, 142-154.
- Merrill, E.H. M.K. Bramble-Brodahl R.W. Marrs and M.S. Boyce. 1993. Estimation of green herbaceous phytomass from Landsat MSS data in Yellowstone National Park. *J. Range Manage.* 46: 151-157.
- NRCS, 1997. *National Range and Pasture Handbook*, Grazing Lands Technology Institute, Natural Resource Conservation Service, United States Department of Agriculture, Washington, D.C., 448 p.
- Nouvellon, Y., D. Lo Seen, S. Rambal, A. Bégué, M.S. Moran, Y.Kerr, and J. Qi, 2000. Time course of radiation use efficiency in a shortgrass ecosystem: Consequences for remotely sensed estimation of primary production, *Remote Sensing of Environment*, 71:43–55.
- Nouvellon, Y., M.S. Moran, D. Lo Seen, R. Bryant, S. Rambal, W.Ni, A. Bégué, A. Chehbouni, W.E. Emmerich, P. Heilman, and J. Qi, 2001. Coupling a grassland ecosystem model with Landsat imagery for a 10-year simulation of carbon and water budgets, *Remote Sensing of Environment*, 78:131–149.
- Price, J.C., 1993. Estimating leaf area index from satellite data, *IEEE Transactions on Geoscience and Remote Sensing*, 31:727–734.
- Price, J.C., and W.C. Bausch, 1995. Leaf area index estimation from visible and near-infrared reflectance data, *Remote Sensing of Environment*, 52:55–65.
- Qi, J., A. Chehbouni, A.R. Huete, Y.H. Kerr, and S. Sorooshian, 1994. A modified soil adjusted vegetation index, *Remote Sensing of Environment*, 48:119–126.
- Reeves M. C., J. C. Winslow, S. W. Running, 2002, MAPPING WEEKLY RANGELAND VEGETATION PRODUCTIVITY USING MODIS DATA, First Virtual Global Conference on Organic Beef Cattle Production
- Richardson, A.J., J.H. Everitt, and H.W. Gausman, 1983. Radiometric estimation of biomass and nitrogen content of Alicia grass, *Remote Sensing of Environment*, 13:179–184.
- Tucker C.J., C.L. Vanparet, and A. Gaston. 1983. Satellite remote sensing of total dry matter production in the Senegalese Sahel. *Remote Sens. Environ.* 17:233-249.
- Tueller, P.T. 1989. Remote sensing technology for rangeland management. *J. Range Manage.* 42:442-452.
- Kennedy, P. 1989. Monitoring the vegetation of Tunisian grazing lands using the normalized difference vegetation index. *Ambio* 18: 119-123.
- Thoma, D. 1998. Near Real-Time Satellite and Ground Based Radiometric Estimation of Vegetation Biomass, and Nitrogen Content in Montana Rangelands. MS Thesis. Montana State University, Bozeman Mont.

- Tucker, C.J., C. Vanpraet, E. Boerwinkel, and A. Gaston, 1983. Satellite remote sensing of total dry matter production in the Senegalese sahel, *Remote Sensing of Environment*, 13:461–474.
- Tueller, 1989. Remote sensing technology for rangeland management applications, *Journal of Range Management*, 42:442–453.
- Reeves, M.C., J.C. Winslow, and S.W. Running, 2001. Mapping weekly rangeland vegetation productivity, *Journal of Range Management*, 54(suppl):A90–A105.
- Washington-Allen, R.A., N.E. West, R.D. Ramsey, and C.T. Hunsaker, 1999. Characterization of the ecological integrity of commercially grazed rangelands using remote sensing-based ecological indicators, *Proceedings of the VI International Rangelands Congress: People and Rangelands, Building the Future* (D. Eldridge and D. Freudenberger, editors), 17-23 July, Townsville, Queensland, Australia (VI International Rangeland Congress, Aitkenvale, Queensland, Australia), 2:778–780.
- Wylie, B.K., I. Dendra, R.D. Piper, J.A. Harrington, B.C., Reed, and G.M., Southward. 1995. Satellite-Based herbaceous biomass estimates in the pastoral zone of Niger. *J. Range Manage.* 48: 159-164.

Table 1. Climatic attributes of some synoptic and climatologically stations inside the Yazd-Ardakan plain

| Station/ Parameter | Ardakan | Meybod | Chah Afzal | Ashkezar | Ebrahim Abad | Mehriz | Aqda | Yazd |
|-----------------------|---------|--------|---------------|----------|-----------------|--------|------|------|
| T _{mean} | 19.2 | 19 | 19.3 | 19.1 | 17.9 | 19.1 | 20.8 | 20.2 |
| P _{mean} | 60.3 | 45.1 | 46.6 | 50.3 | 63.4 | 63.2 | 79.6 | 51.9 |

Table 2. List of acquired MODIS data that were used in this study

| Year | Jan | Feb | Mar | Apr | May | Jun | Jul | Aug | Sep | Oct | Nov | Dec |
|------|-----|-----|-----|-----|-----|-----|-----|-----|-----|-----|-----|-----|
| 2000 | | | * | * | * | * | * | | | | | |
| 2001 | | | | * | * | * | | | | | | |
| 2002 | | | | * | * | * | | | | | | |
| 2003 | | | | * | * | * | | | | | | |
| 2004 | | | | * | * | * | | | | | | |
| 2005 | | | | * | * | * | | | | | | |
| 2006 | | | | * | * | * | | | | | | |
| 2007 | | | * | * | * | * | * | * | * | | | |
| 2008 | | | | * | * | * | | | | | | |
| 2009 | | | | * | * | * | | | | | | |

Table 3. List of different vegetation indices that were derived from MODIS[§] products

| No. | Index | Description | Formula |
|-----|---------------------------------------|---|---|
| 1 | DVI (Tucker, 1979) | Difference Vegetation Index | NIR - R |
| 2 | fPAR (Fensholt et al 2004) | fractional Photosynthetically Active Radiation | 1.51 NDVI _{modis} -0.4 |
| 3 | IPVI (Crippen, 1990) | Infra-red Percentage Vegetation Index | NIR / (NIR + R) |
| 4 | MSAVI (Qi et al. (1994a) | Modified Soil Adjusted Vegetation Index | $\frac{NIR - R}{NIR + R + L} (1 + L)$; L = 1 - 2 * γ * NDVI * WDWI γ = slope of soil line = Arc tan(a) |
| 5 | MSAVI ₂ (Qi et al. (1994b) | 2 nd Modified Soil Adjusted Vegetation Index | $\frac{(2 * NIR) + 1 - \sqrt{(2 * NIR + 1)^2 - 8 * (NIR - R)}}{2}$ |
| 6 | PVI (Jackson, 1983) | Perpendicular Vegetation Index | 0.647 * NIR - 0.763 * R - 0.02 |
| 7 | RVI (Jordan, 1969) | Ratio Vegetation Index | $\frac{NIR}{R}$ |
| 8 | SAVI (Huete, 1988) | Soil Adjusted Vegetation Index | $\frac{NIR - R}{NIR + R + L} (1 + L)$ L=0.5 |
| 9 | WDVI (Clevers, 1988) | Weighted Difference Vegetation Index | WDVI = NIR - γ * R γ = slope of soil line = Arc tan(a) |
| 10 | NDVI (Rouse et al. ,1973) | Normalized Difference Vegetation Index | $\frac{NIR - R}{NIR + R}$ |

§: In MODIS products, reflectance values of band1 and band2 represent Red and NIR ranges of spectrum, respectively

Table 4. Correlation coefficient (R^2) matrix between climatic parameters and different vegetation indices for Yazd-Ardakan rangeland*

| Index | P | T | H | WS | SPI | DVI | fPAR | IPVI | MSAVI | MSAVI2 | NDVI | PVI | RVI | SAVI | WDVI |
|--------|---|---|------|------|------|------|------|------|-------|--------|------|------|------|-------------|------|
| P | 1 | 0 | 0.03 | 0.02 | 1 | 0.31 | 0.21 | 0.22 | 0.41 | 0.00 | 0.02 | 0.20 | 0.02 | <u>0.82</u> | 0.04 |
| T | | 1 | 0.76 | 0.00 | 0.00 | 0.31 | 0.18 | 0.06 | 0.21 | 0.01 | 0.03 | 0.09 | 0.02 | <u>0.36</u> | 0.25 |
| H | | | 1 | 0.05 | 0.03 | 0.15 | 0.05 | 0.00 | 0.26 | 0.01 | 0.23 | 0.38 | 0.23 | 0.05 | 0.06 |
| WS | | | | 1 | 0.02 | 0.07 | 0.01 | 0.06 | 0.06 | 0.00 | 0.09 | 0.02 | 0.12 | 0.12 | 0.00 |
| SPI | | | | | 1 | 0.31 | 0.20 | 0.22 | 0.41 | 0.00 | 0.02 | 0.20 | 0.02 | <u>0.82</u> | 0.04 |
| DVI | | | | | | 1 | 0.00 | 0.64 | 0.94 | 0.40 | 0.15 | 0.00 | 0.15 | 0.14 | 0.63 |
| fPAR | | | | | | | 1 | 0.10 | 0.10 | 0.34 | 0.55 | 0.84 | 0.55 | 0.46 | 0.05 |
| IPVI | | | | | | | | 1 | 0.48 | 0.54 | 0.21 | 0.08 | 0.21 | 0.07 | 0.53 |
| MSAVI | | | | | | | | | 1 | 0.21 | 0.03 | 0.02 | 0.04 | 0.26 | 0.46 |
| MSAVI2 | | | | | | | | | | 1 | 0.62 | 0.47 | 0.60 | 0.01 | 0.64 |
| NDVI | | | | | | | | | | | 1 | 0.85 | 0.99 | 0.39 | 0.33 |
| PVI | | | | | | | | | | | | 1 | 0.84 | 0.60 | 0.12 |
| RVI | | | | | | | | | | | | | 1 | 0.40 | 0.32 |
| SAVI | | | | | | | | | | | | | | 1 | 0.02 |
| WDVI | | | | | | | | | | | | | | | 1 |

*: In this table P is precipitation, T is temperature, H is humidity, WS is wind speed, SPI is standardized precipitation index and other indicators are different remotely sensed vegetation indices

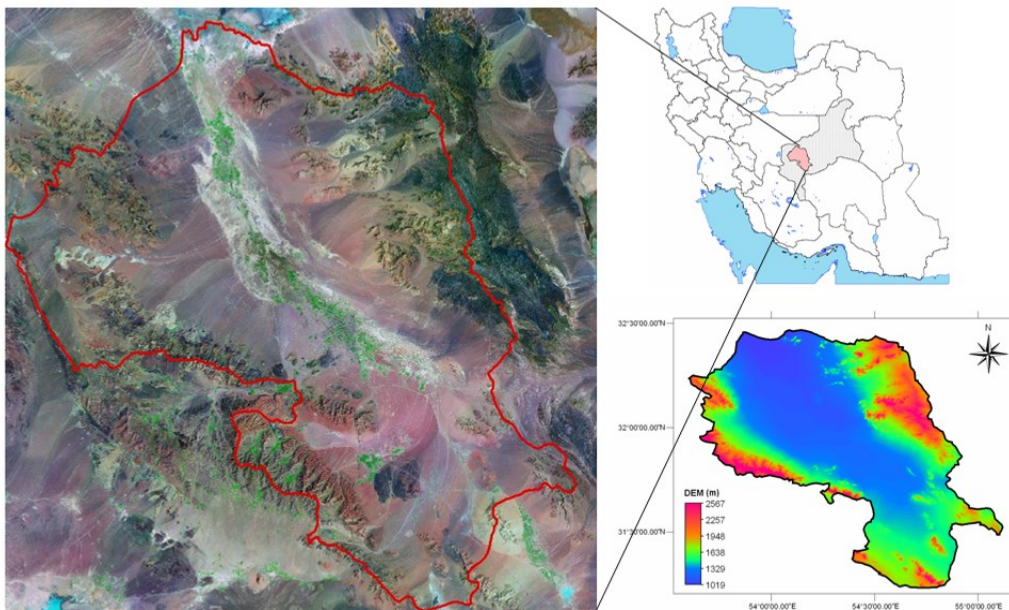


Fig1. Satellite image of Yazd Ardakan plain in Yazd province, central Iran, and also its digital elevation model (DEM)

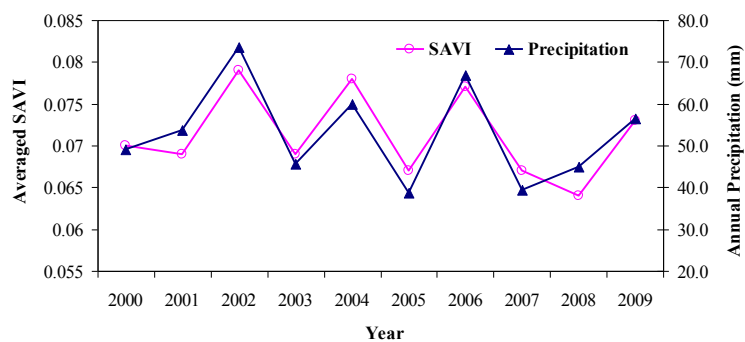


Fig 2. Temporal changes of annual precipitation and SAVI indicators in Yazd-Ardakan rangeland

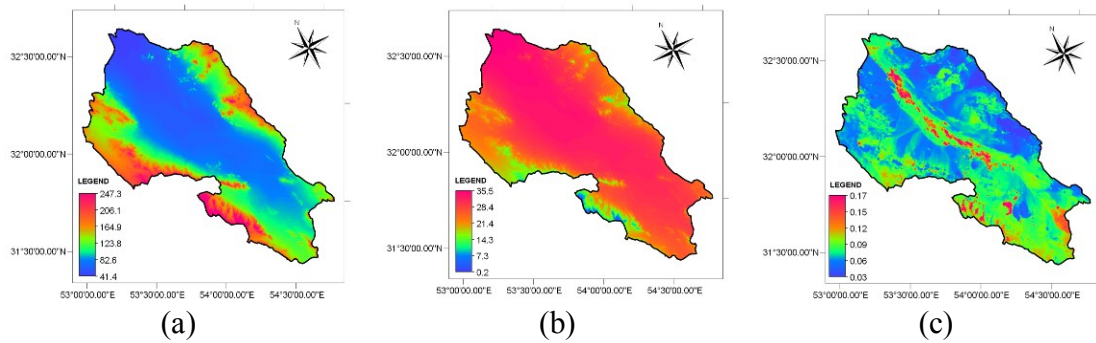


Fig 3. Averaged (a) annual precipitation, (b) annual temperature and (c) Soil Adjusted Vegetation Index (SAVI) maps of Yazd-Ardakan plain in a decade (2000-2009)

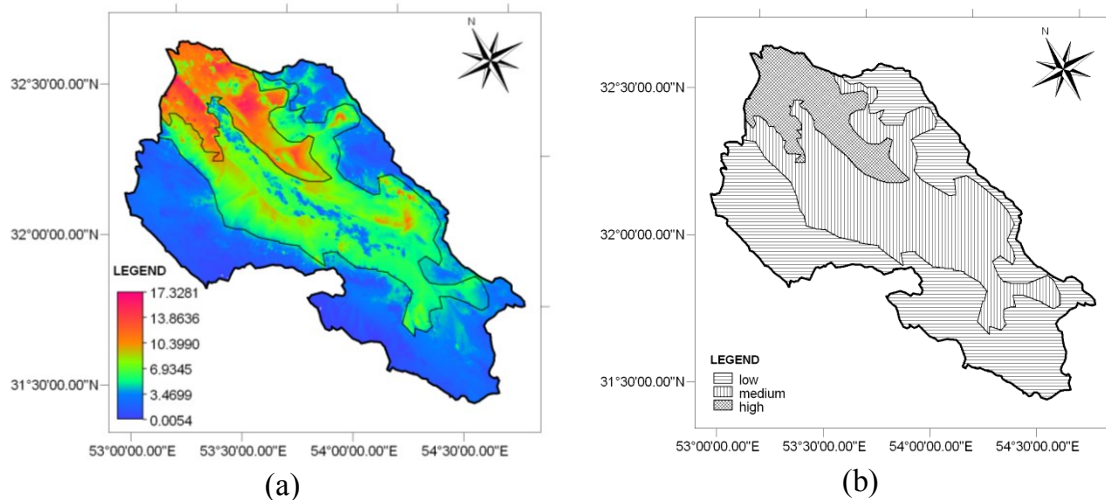


Fig4. (a) Impact factor map and (b) its classification in Yazd-Ardakan plain

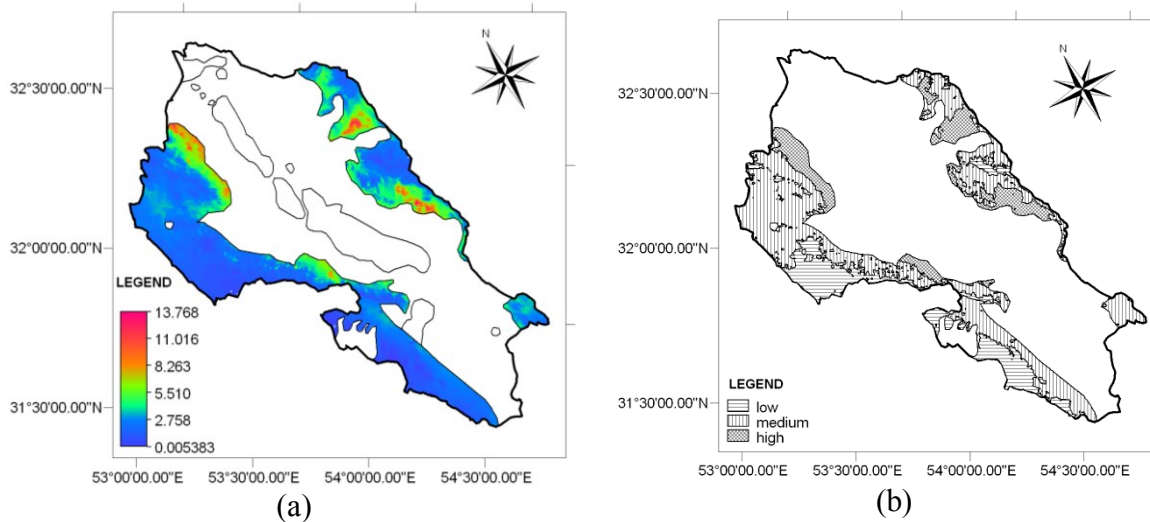


Fig5. (a) Impact factor map and (b) its classification in rangeland areas of Yazd-Ardakan plain